Supporting Information

Enhanced all-climate sodium-ion batteries performance in a low-defect and Na-enriched Prussian blue analogue cathode by nickel substitution

Jingwen Zhang[1], Jing Wan[2], Mingyang Ou[1], Siying Liu[1], Bicheng Huang[1], Jia Xu[1], Shixiong Sun[1], Yue Xu[1], Yaqing Lin[1,*], Chun Fang[1,*] Jiantao Han[1]

[1]State Key Laboratory of Material Processing and Die & Mould Technology, School of Materials Science and Engineering, Huazhong University of Science and Technology, Wuhan 430074, Hubei, China.
[2]Department of Applied Physics, Chongqing University, Chongqing 401331, China.

***Correspondence to:** Yaqing Lin, State Key Laboratory of Material Processing and Die & Mould Technology, School of Materials Science and Engineering, Huazhong University of Science and Technology, Wuhan 430074, Hubei, China. E-mail: 359702366@qq.com; Dr. Assoc. Prof. Chun Fang, a State Key Laboratory of Material Processing and Die & Mould Technology, School of Materials Science and Engineering, Huazhong University of Science and Technology, Wuhan 430074, Hubei, China. E-mail: fangchun@hust.edu.cn

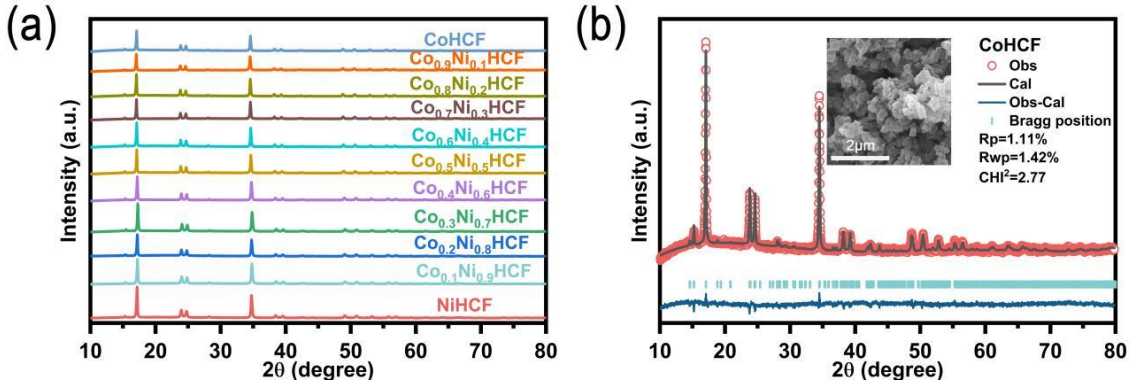

Supplementary Figure 1. (a) XRD patterns of $Co_xNi_{1-x}HCF$ with different ratios of Co^{2+}: Ni^{2+} from 10: 0 to 0: 10, respectively. (b) Rietveld refinements of the structures of the CoHCF.

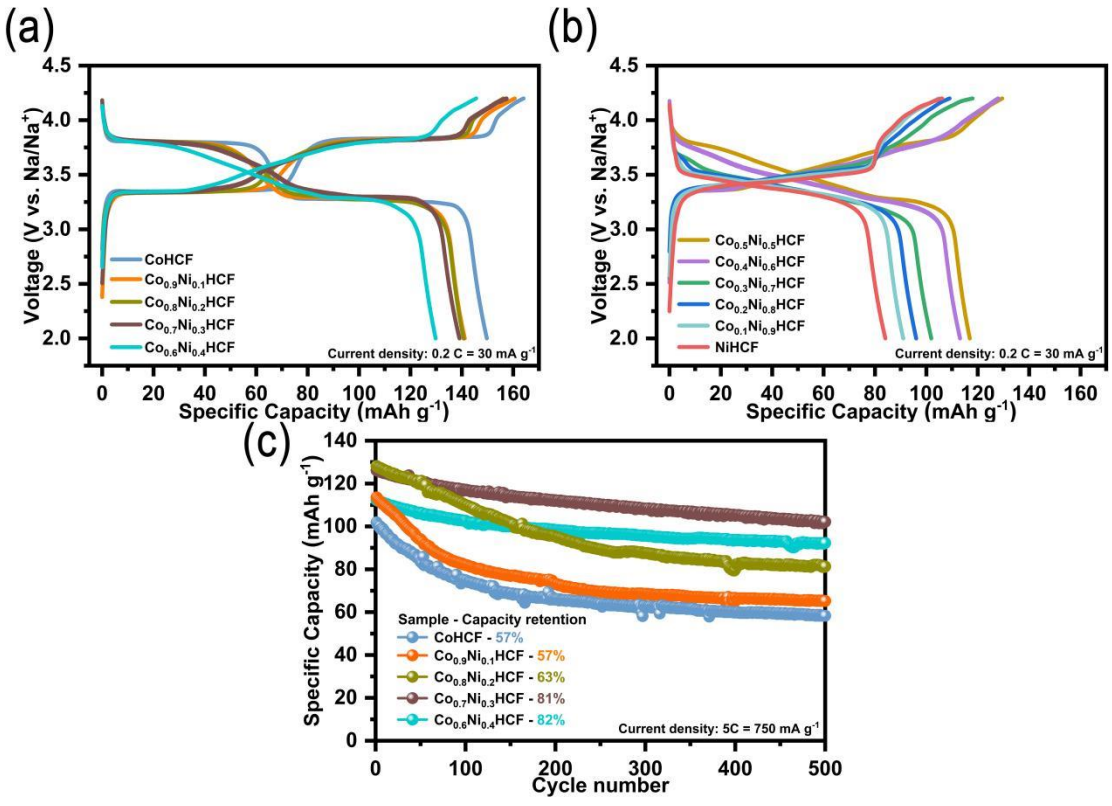

Supplementary Figure 2. (a, b) Charge/discharge voltage profiles of $Co_xNi_{1-x}HCF$ with different ratios of Co^{2+}: Ni^{2+} from 10: 0 to 0: 10 at a current density of 30 mA g^{-1}, respectively. (c) Cycling performance and capacity retention after 500 cycles at a current density range of 750 mA g^{-1} of $Co_xNi_{1-x}HCF$ (x=1.0, 0.9, 0.8, 0.7, 0.6).

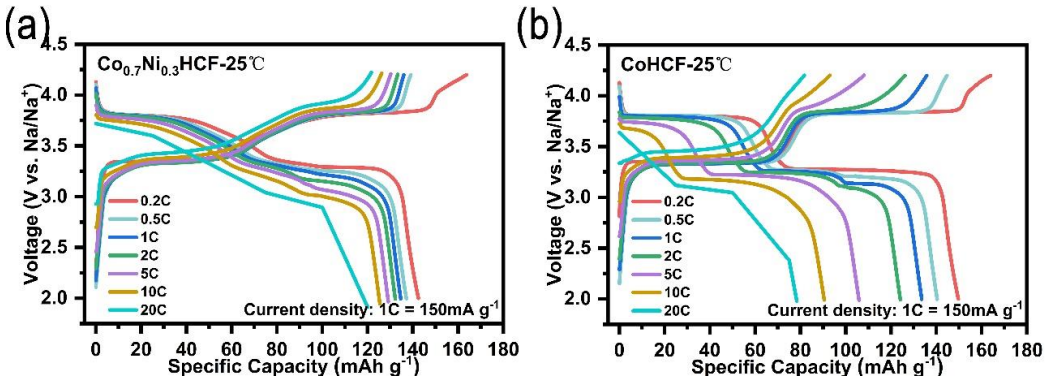

Supplementary Figure 3. Charge/discharge voltage profiles of (a) $Co_{0.7}Ni_{0.3}HCF$ and (b) CoHCF at different rates.

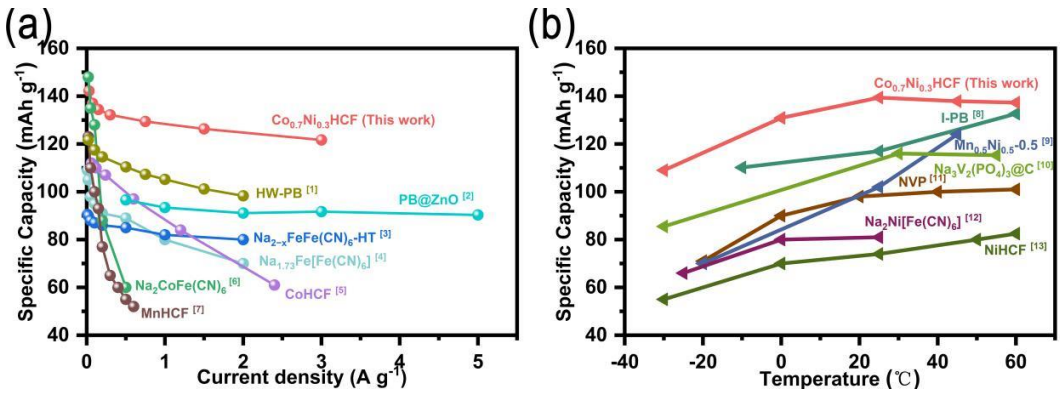

Supplementary Figure 4. (a) Rate performance and (b) All-climate electrochemical performance of $Co_{0.7}Ni_{0.3}HCF$ in this work compared to previously reported Prussian blue cathode materials.

References:

1. Hu J, Tao H, Chen M, et al. Interstitial Water Improves Structural Stability of Iron Hexacyanoferrate for High-Performance Sodium-Ion Batteries. *ACS Appl Mater Interfaces* 2022; 14: 12234-42. [DOI: 10.1021/acsami.1c23762]

2. Qiao Y, Wei G, Cui J, et al. Prussian blue coupling with zinc oxide as a protective layer: an efficient cathode for high-rate sodium-ion batteries. *Chem Commun (Camb)* 2019; 55: 549-52. [DOI: 10.1039/c8cc07951j]

3. Wang W, Gang Y, Peng J, et al. Effect of Eliminating Water in Prussian Blue Cathode for Sodium-Ion Batteries. *Adv Funct Mater* 2022; 32: 2111727. [DOI: 10.1002/adfm.202111727]

4. Wang W, Gang Y, Hu Z, et al. Reversible structural evolution of sodium-rich

rhombohedral Prussian blue for sodium-ion batteries. *Nat Commun* 2020; 11: 980. [DOI: 10.1038/s41467-020-14444-4]

5. Shao T, Li C, Liu C, et al. Electrolyte regulation enhances the stability of Prussian blue analogues in aqueous Na-ion storage. *J Mater Chem A* 2019; 7: 1749-55. [DOI: 10.1039/c8ta10860a]

6. Wu X, Wu C, Wei C, et al. Highly Crystallized Na(2)CoFe(CN)(6) with Suppressed Lattice Defects as Superior Cathode Material for Sodium-Ion Batteries. *ACS Appl Mater Interfaces* 2016; 8: 5393-9. [DOI: 10.1021/acsami.5b12620]

7. Tang Y, Li W, Feng P, et al. Investigation of alkali-ion (Li, Na and K) intercalation in manganese hexacyanoferrate KxMnFe(CN)6 as cathode material. *Chem Eng J* 2020; 396: 125269. [DOI: 10.1016/j.cej.2020.125269]

8. Peng J, Zhang W, Hu Z, et al. Ice-Assisted Synthesis of Highly Crystallized Prussian Blue Analogues for All-Climate and Long-Calendar-Life Sodium Ion Batteries. *Nano Lett* 2022; 22: 1302-10. [DOI: 10.1021/acs.nanolett.1c04492]

9. Xu Z, Sun Y, Xie J, et al. Scalable Preparation of Mn/Ni Binary Prussian Blue as Sustainable Cathode for Harsh-Condition-Tolerant Sodium-Ion Batteries. *ACS Sustain Chem Eng* 2022; 10: 13277-87. [DOI: 10.1021/acssuschemeng.2c02377]

10. Liu T, Wang B, Gu X, et al. All-climate sodium ion batteries based on the NASICON electrode materials. *Nano Energy* 2016; 30: 756-61. [DOI: 10.1016/j.nanoen.2016.09.024]

11. Liu X, Zheng X, Qin X, et al. Temperature-responsive solid-electrolyte-interphase enabling stable sodium metal batteries in a wide temperature range. *Nano Energy* 2022; 103A: 107746. [DOI: 10.1016/j.nanoen.2022.107746]

12. Ma X, Wei Y, Wu Y, et al. High crystalline Na2Ni[Fe(CN)(6)] particles for a high-stability and low-temperature sodium-ion batteries cathode. *Electrochimica Acta* 2019; 297: 392-7. [DOI: 10.1016/j.electacta.2018.11.063]

13. Sun Y, Xu Y, Xu Z, et al. Long-life Na-rich nickel hexacyanoferrate capable of working under stringent conditions. *J Mater Chem A* 2021; 9: 21228-40. [DOI: 10.1039/d1ta05998j]

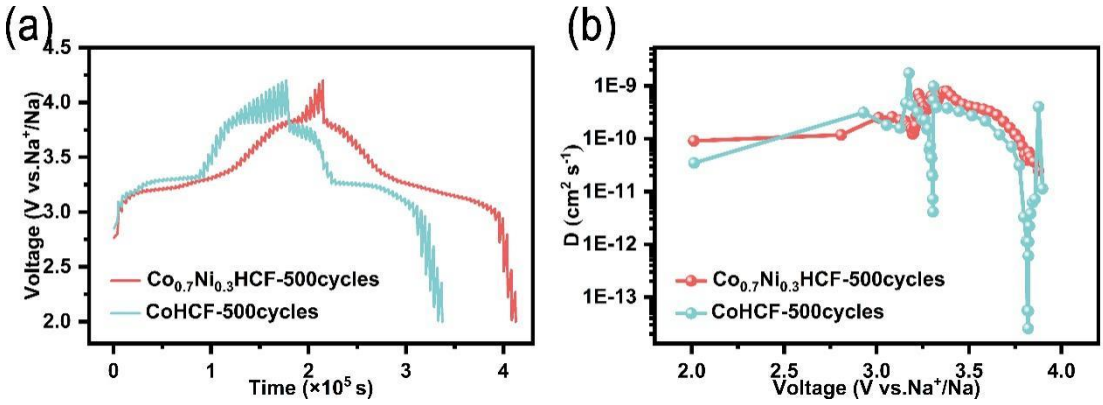

Supplementary Figure 5. (a) GITT curves of samples. (b) Calculated Na^+-ions diffusion coefficients (D_{Na^+}) of samples after 500 cycles at a current density of 750 mA g^{-1} from the GITT tests during the charging process.

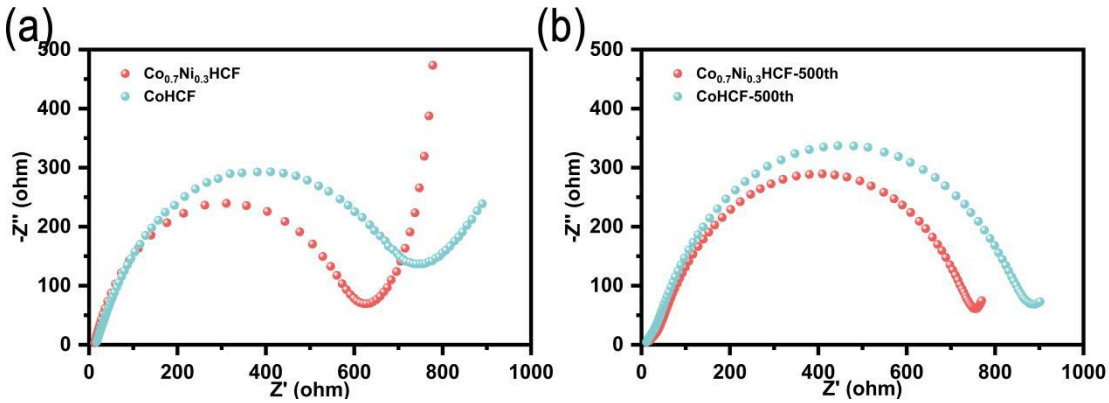

Supplementary Figure 6. Electrochemical impedance spectra of the electrodes at the (a) fresh, (b) 500th in the frequency range of 100 kHz-0.01 Hz.

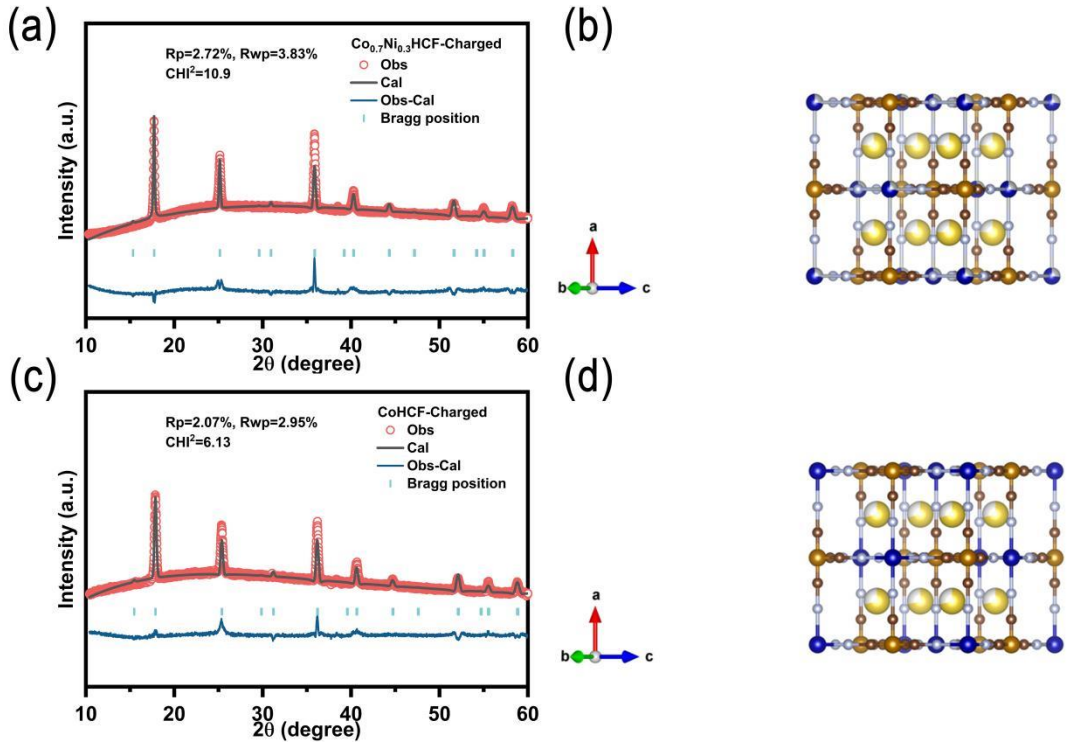

Supplementary Figure 7. The Rietveld refinements of cubic phase (Charged) (a) $Co_{0.7}Ni_{0.3}HCF$, (c) CoHCF and schematic illustrations of the structures of the (b) $Co_{0.7}Ni_{0.3}HCF$, (d) CoHCF.

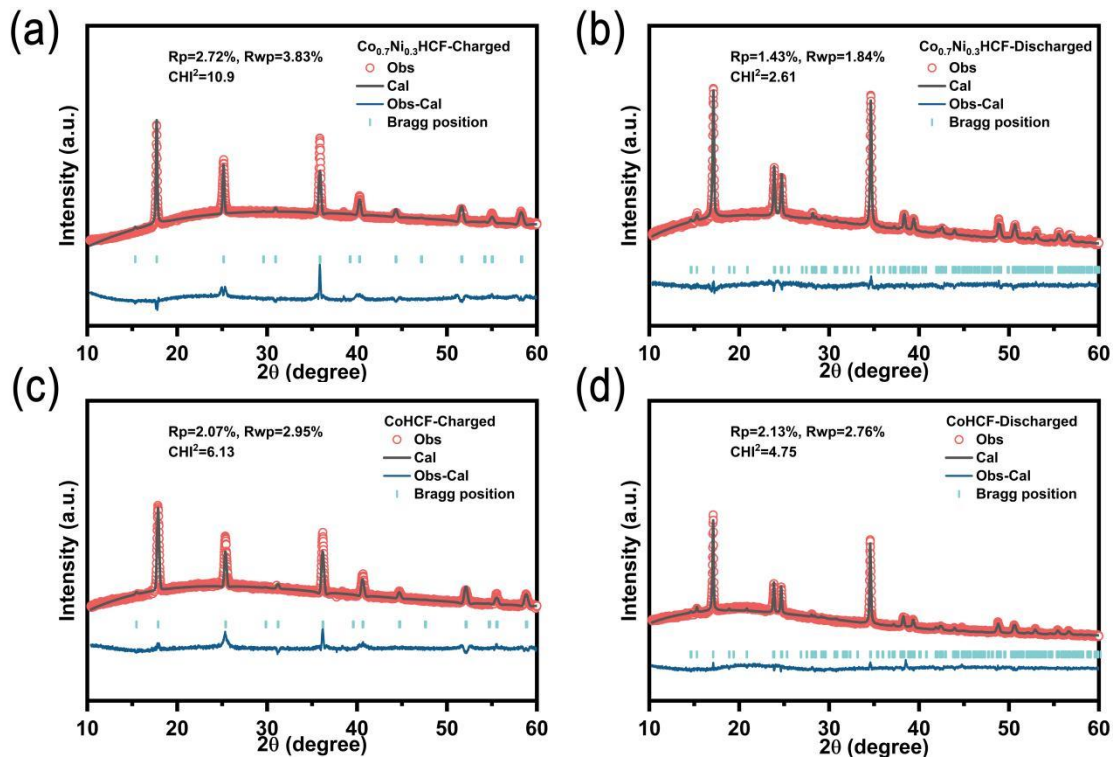

Supplementary Figure 8. The Rietveld refinements of cubic phase (Charged) (a)

$Co_{0.7}Ni_{0.3}HCF$, (c) CoHCF and monoclinic phase (Discharged) (b) $Co_{0.7}Ni_{0.3}HCF$, (d) CoHCF.

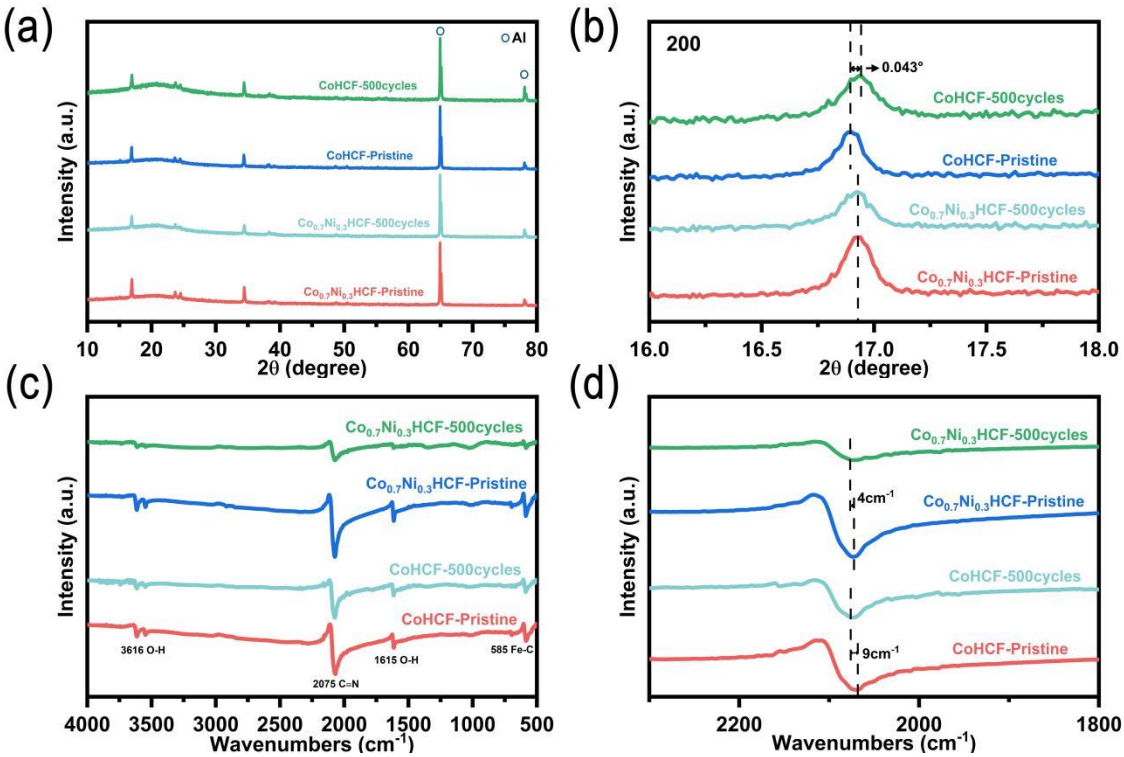

Supplementary Figure 9. (a, b) XRD patterns and (c, d) FTIR spectra of $Co_{0.7}Ni_{0.3}HCF$ and CoHCF at a current density of 750 mA g^{-1} at different cycles (Pristine and 500 cycles).

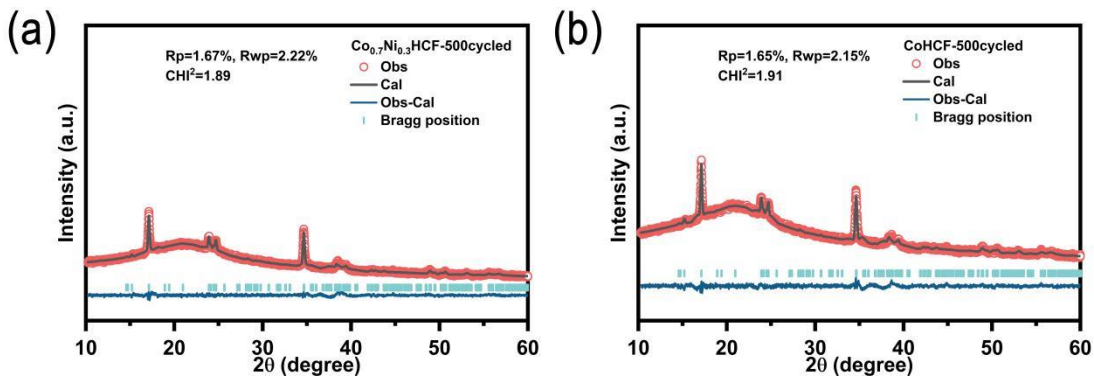

Supplementary Figure 10. The Rietveld refinements of (a) $Co_{0.7}Ni_{0.3}HCF$ and (b) CoHCF after 500 cycles.

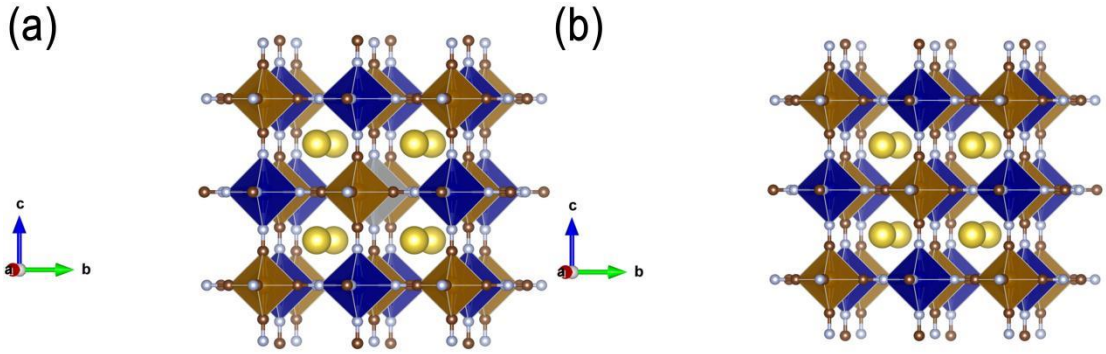

Supplementary Figure 11. Schematic illustrations of the structures of (a) $Co_{0.7}Ni_{0.3}HCF$ and (b) CoHCF unit cell of calculation model.

Supplementary Table 1. Structural parameters of $Co_{0.7}Ni_{0.3}HCF$ and CoHCF obtained from Rietveld analysis.

$Co_{0.7}Ni_{0.3}HCF$

P21/n a=10.3656(5) Å, b=7.4286(4) Å, c=7.2269(4) Å, α=γ=90°, β=92.805(3) °. Rp=0.976%, Rwp=1.32%, CHI^2=2.14					
Atom	x	y	z	Occ.	Wyckoff
Na	0.29038	0.46415	-0.00330	1.007	4e
Co1	0.50000	0.50000	0.50000	0.826	2a
Ni1	0.50000	0.50000	0.50000	0.174	2a
Fe1	0.50000	0.00000	1.00000	0.984	2d
N1	0.51415	0.29317	0.71358	0.977	4e
N2	0.28183	0.50057	0.49977	0.977	4e
N3	0.49884	0.29810	0.30142	0.977	4e
C1	0.50065	0.19069	0.80104	0.977	4e
C2	0.20597	0.49610	0.51355	0.977	4e
C3	0.49862	0.19991	0.18453	0.977	4e
O1	0.27235	0.24128	0.26981	1.024	4e

CoHCF

P21/n a=10.4118(7) Å, b=7.4573(5) Å, c=7.2608(5) Å, α=γ=90°, β=92.730(4) °. **Rp=1.11%, Rwp=1.42%, CHI^2=2.77**					
Atom	x	y	z	Occ.	Wyckoff
Na	0.29326	0.45958	-0.00310	0.972	4e
Co1	0.50000	0.50000	0.50000	1	2a
Fe1	0.50000	0.00000	1.00000	0.992	2d
N1	0.51968	0.30804	0.72035	0.999	4e
N2	0.27972	0.51164	0.49766	0.999	4e
N3	0.49967	0.30385	0.28843	0.999	4e
C1	0.51349	0.21051	0.79955	0.999	4e
C2	0.20427	0.50592	0.49984	0.999	4e
C3	0.50299	0.18615	0.18800	0.999	4e
O1	0.29437	0.24498	0.26794	1.026	4e

Supplementary Table 2. Structural parameters of $Co_{0.7}Ni_{0.3}$HCF-Charged(Cubic) and CoHCF-Charged(Cubic) obtained from Rietveld analysis.

$Co_{0.7}Ni_{0.3}$HCF-Charged

Fm-3m a=b=c=10.0154(3) Å, α=β=γ=90.0000 °, **Rp=2.72%, Rwp=3.83%, CHI^2=10.9**					
Atom	x	y	z	Occ.	Wyckoff
Na	0.75000	0.75000	0.75000	0.756	8c
Ni1	0.50000	1.00000	0.50000	0.27	4a
Co1	0.50000	1.00000	0.50000	0.733	4a
Fe1	0.50000	0.50000	0.50000	1.000	4b
N1	0.50000	0.78878	0.50000	1.000	24e
C1	0.50000	0.64663	0.50000	1.000	24e
O1	0.50000	0.75000	0.75000	0.756	8c

CoHCF-Charged

Fm-3m a=b=c=9.9297(3) Å, α=β=γ=90.0000 °, **Rp=2.07%, Rwp=2.95%, CHI^2=6.13**					
Atom	x	y	z	Occ.	Wyckoff
Na	0.75000	0.75000	0.75000	0.711	8c
Co1	0.50000	1.00000	0.50000	1.009	4a
Fe1	0.50000	0.50000	0.50000	1.000	4b
N1	0.50000	0.79383	0.50000	1.000	24e
C1	0.50000	0.64526	0.50000	1.000	24e
O1	0.50000	1.00000	0.74648	0.526	24e

Supplementary Table 3. The lattice parameters of $Co_{0.7}Ni_{0.3}$HCF and CoHCF in stage of charging and discharging.

Sample	**Compositions (based on ICP-OES and TG)**	**Statement Lattice parameters**
$Co_{0.7}Ni_{0.3}$HCF	$Na_{2.008}Ni_{0.269}Co_{0.731}[Fe(CN)_6]_{0.997}$•2.09$H_2O$ **Rate=10.78%**	**Charged (Cubic)** Rp=2.72% Rwp=3.83% CHI^2=10.9 a=b=c=10.0154(3)
		α=β=γ=90°
		V=1004.63(6)
		Discharged (Monoclinic) Rp=1.43% Rwp=1.84% CHI^2=2.61 a=10.3678(9), b=7.4284(7)

		c= 7.2339(6)
		α=γ=90°, β= 92.776(6)°
		V=556.47(9)
CoHCF	$Na_{2.047}Co[Fe(CN)_6]_{0.997}•2.19H_2O$ **Rate=14.27%**	**Charged (Cubic)** Rp=2.07% Rwp=2.95% CHI^2=6.13 a=b=c=9.9297(3)
		α=β=γ=90°
		V=979.07(6)
		Discharged (Monoclinic) Rp=2.13% Rwp=2.76% CHI^2=4.75 a=10.3868(12), b=7.4822(9)
		c= 7.2047(8)
		α=γ=90°, β=92.543(7)°
		V=559.37(11)

The volume change rate during the two-phase phase transition is calculated by Formula [27]:

$$\text{Rate} = \frac{2*V_{\text{Discharged}} - V_{\text{charged}}}{V_{\text{charged}}} * 100\%$$

27. Hu J, Tao H, Chen M, et al. Interstitial Water Improves Structural Stability of Iron Hexacyanoferrate for High-Performance Sodium-Ion Batteries. *ACS Appl Mater Interfaces* 2022; 14: 12234-42. [DOI: 10.1021/acsami.1c23762]

Supplementary Table 4. The lattice parameters of $Co_{0.7}Ni_{0.3}$HCF and CoHCF before and after 500 cycles.

sample	a (Å)	b (Å)	c (Å)	β (°)	Occ. (Na)	V (Å^3)
$Co_{0.7}Ni_{0.3}$HCF-pristine	10.3656(5)	7.4286(4)	7.2269(4)	92.805(3)	1.007	555.81(5)
$Co_{0.7}Ni_{0.3}$HCF-500cycled	10.3639(17)	7.3707(15)	7.2808(14)	92.607(12)	0.999	555.60(18)
CoHCF-pristine	10.4118(7)	7.4573(5)	7.2608(5)	92.730(4)	0.972	563.13(6)
CoHCF-500cycled	10.3709(18)	7.3777(16)	7.2846(15)	92.586(14)	0.933	556.80(19)

The volume change rate of $Co_{0.7}Ni_{0.3}$HCF and CoHCF after 500 cycles is calculated by Formula:

$$\text{rate} = \frac{V_{pristine} - V_{cycled}}{V_{pristine}} * 100\%$$